Search for the baryon- and lepton-number violating decays $B^0 \to p\mu^-$ and $B_s^0 \to p\mu^-$

R. Aaij *et al.*[*]

(LHCb Collaboration)

A search for the baryon- and lepton-number violating decays $B^0 \to p\mu^-$ and $B_s^0 \to p\mu^-$ is performed at the LHCb experiment using data collected in proton-proton collisions at $\sqrt{s} = 7$, 8 and 13 TeV, corresponding to integrated luminosities of 1, 2, and 6 fb^{-1}, respectively. No significant signal for $B^0 \to p\mu^-$ and $B_s^0 \to p\mu^-$ decays is found and the upper limits on the branching fractions are determined to be $\mathcal{B}(B^0 \to p\mu^-) < 2.6(3.1) \times 10^{-9}$ and $\mathcal{B}(B_s^0 \to p\mu^-) < 12.1(14.0) \times 10^{-9}$, respectively, at 90% (95%) confidence level. These are the first limits on these decays to date.

I. INTRODUCTION

Despite the tremendous success of the Standard Model (SM) of particle physics in the past few decades, there are still some important questions that are not answered. One of them is the observation of the matter-antimatter asymmetry in the Universe, which brings a serious challenge to our understanding of nature. In 1967, Andrei Sakharov proposed three necessary conditions that must be satisfied to produce such a large matter-antimatter asymmetry, one of which is baryon number violation (BNV) [1]. Various extensions of the SM that include BNV processes, known as grand unified theory (GUT) models, have been proposed, such as SU(5) [2], SO(10) [3], E_6 [4], and flipped SU(5) [5,6]. These GUT models usually require two hypothetical gauge bosons, X and Y, with electric charges of $\pm\frac{4}{3}e$ and $\pm\frac{1}{3}e$, that couple quarks to leptons and lead to both BNV and lepton number violation (LNV).

Proton decay is a BNV process of the lightest baryon: none of its decay modes, although predicted by many GUT models, have been observed [7]. However, since proton decay only involves first-generation quarks, experimental searches for BNV decays of heavy-flavor hadrons are very important and represent additional probes for new physics effects. Various BNV processes have been searched for in τ, Λ, D, J/ψ, and B decays by the CLEO [8], CLAS [9], BESIII [10–13], and *BABAR* [14] experiments, but no evidence has been found so far. The large data samples accumulated by the LHCb experiment are expected to lead

to the best sensitivity for investigating BNV decays of B mesons. The $B_{(s)}^0 \to p\ell^-$ decay modes, with possible hypothetical Feynman diagrams shown in Fig. 1, are relevant BNV and LNV processes that are forbidden in the SM with a prediction of $\mathcal{B}(\bar{b} \to uu\ell^-) < 2.4 \times 10^{-27}$ [15] derived from the constraint of proton stability.

In this paper, we present the first search for $B^0 \to p\mu^-$ and $B_s^0 \to p\mu^-$ decays[1] using proton-proton ($p\,p$) collisions collected with the LHCb detector and corresponding to an integrated luminosity of 1 fb^{-1} at a center-of-mass energy $\sqrt{s} = 7$ TeV, 2 fb^{-1} at $\sqrt{s} = 8$ TeV, and 6 fb^{-1} at $\sqrt{s} = 13$ TeV. The first two datasets are referred to as run 1 and as run 2. Two normalization channels are used: the $B^0 \to K^+\pi^-$ decay, which has a similar topology to that of the signal, and the $B^+ \to J/\psi(\mu^+\mu^-)K^+$ decay, due to its high abundance and the high purity that can be achieved at the LHCb experiment. The $B_{(s)}^0 \to p\mu^-$ candidates with $p\mu^-$ pair invariant mass $m_{p\mu^-}$ in the range [5067, 5667] MeV/c^2 are selected. To avoid potential biases, $B_{(s)}^0 \to p\mu^-$ candidates in the signal region, $m_{p\mu^-} \in [5217, 5457]$ MeV/c^2, were not examined until the selection and fitting procedure were finalized.

II. DETECTOR AND SIMULATION

The LHCb detector [16,17] is a single-arm forward spectrometer covering the pseudorapidity range $2 < \eta < 5$, designed for the study of particles containing b or c quarks. The detector includes a high-precision tracking system consisting of a silicon-strip vertex detector surrounding the

---

[*]Full author list given at the end of the article.

[1]$B_{(s)}^0 \to p\mu^-$ represents $B_{(s)}^0 \to p\mu^-$ and $\bar{p}\mu^+$ and the inclusion of charge-conjugate processes is implied throughout this paper, unless otherwise noted.

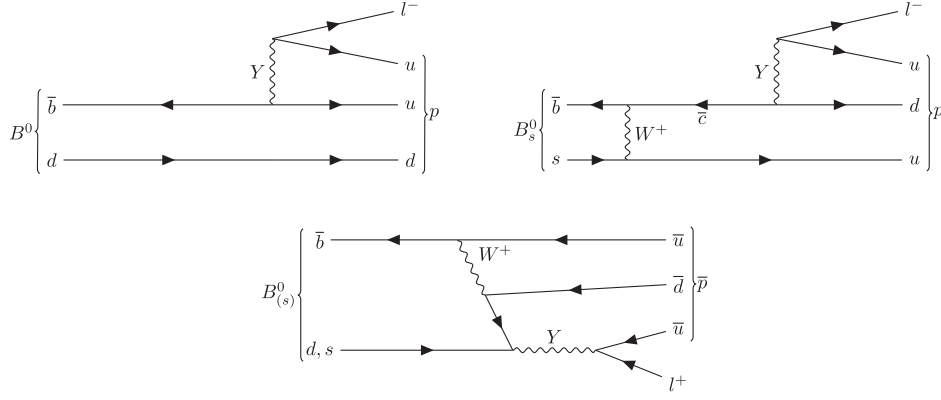FIG. 1.   Hypothetical Feynman diagrams of $B^0_{(s)} \to p\ell^-$ and $\bar{p}\ell^+$ mediated by a hypothetical Y boson.

$p\,p$ interaction region, a large-area silicon-strip detector located upstream of a dipole magnet with a bending power of about 4 Tm, and three stations of silicon-strip detectors and straw drift tubes placed downstream of the magnet. The tracking system provides a measurement of momentum, p, of charged particles with a relative uncertainty that varies from 0.5% at low momentum to 1.0% at 200 GeV/c. The minimum distance of a track to a primary vertex (PV), the impact parameter (IP), is measured with a resolution of $(15 + 29/p_T)$ μm, where p_T is the component of the momentum transverse to the beam, in GeV/c. Different types of charged hadrons are distinguished using information from two ring-imaging Cherenkov detectors. Photons, electrons, and hadrons are identified by a calorimeter system consisting of scintillating-pad and preshower detectors, an electromagnetic calorimeter and a hadronic calorimeter. Muons are identified by a system composed of alternating layers of iron and multiwire proportional chambers.

The online event selection is performed by a trigger [18], which consists of a hardware stage, based on information from the muon and calorimeter systems, followed by a software stage that applies a full reconstruction of the event. At the hardware stage, the presence of a muon with high p_T is required, while at the software level both tracks are used. A first software stage requires the presence of at least one track with high p_T that is well separated from the PV. It is followed by a second stage that requires a two-track secondary vertex with significant displacement from any PV, and a multivariate algorithm [19,20] is used for the identification of secondary vertices consistent with the decay of a b hadron.

Simulated samples of signal and background channels are used to evaluate geometrical, reconstruction and selection efficiencies, to train multivariate classifiers and to determine the shapes of invariant mass distributions of both signal and background contributions. In the simulation, $p\,p$ collisions are generated using PYTHIA [21] with a specific LHCb configuration [22]. Decays of hadronic particles are described by EvtGen [23], in which final-state radiation is

generated using PHOTOS [24]. The signal events are generated by assuming the $B^0_{(s)}$ decays do not produce any preferred polarization of the proton. The interaction of the generated particles with the detector, and its response, are simulated using the Geant4 toolkit [25,26] as described in Ref. [27].

III. SELECTION

The $B^0_{(s)} \to p\mu^-$ candidates are reconstructed by combining two oppositely charged tracks with transverse momentum in the range $0.25 < p_T < 40$ GeV/c, momentum $p < 500$ GeV/c, as in Ref. [28]. The tracks are also required to have a good track fit quality, with a track fit χ^2 per degree of freedom smaller than three. Only candidate tracks with $\chi^2_{\text{IP}} > 25$ for any PV are selected, where χ^2_{IP} is defined as the difference between the vertex-fit χ^2 of the PV formed with and without the particle in question. The distance of closest approach between the two tracks is required to be below 0.1 mm. The proton candidates are required to be in the geometric acceptance of the LHCb muon stations to mimic the selection of the muon pair of the normalization channel $B^+ \to J/\psi(\mu^+\mu^-)K^+$. This requirement has a negligible effect on the signal efficiency. The two candidate tracks are required to form a secondary vertex with a vertex-fit χ^2 per degree of freedom (χ^2_{vtx}) smaller than nine. Furthermore, the resulting $B^0_{(s)}$ candidates must have a decay time less than nine times the B^0_s lifetime, $\chi^2_{\text{IP}} < 25$ with respect to the PV for which the χ^2_{IP} is minimal and $p_T > 0.5$ GeV/c, to suppress background from random combinations of tracks originating from the PV.

Particles forming the $B^0_{(s)} \to p\mu^-$ candidates are required to be well identified as a proton and a muon [29], using information from the Cherenkov detectors, the calorimeters and the muon stations. The stringent requirements on the p and μ candidates retain more than 60% of the signal candidates and eliminate more than 99% of the background candidates from decays with misidentified particles,
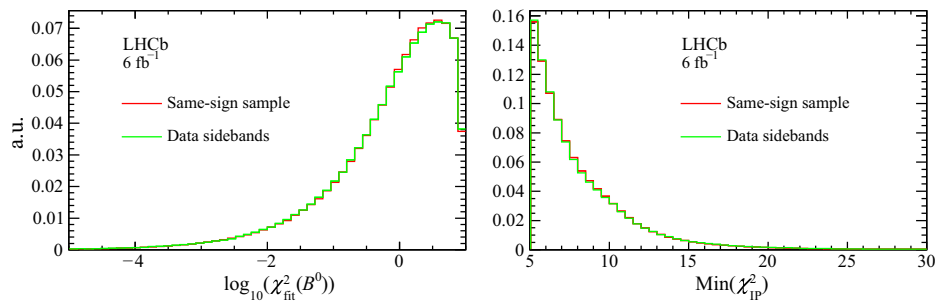
FIG. 2. Comparison of the distributions of the B^0 vertex fit χ^2 $[\chi^2_{\text{fit}}(B^0)]$ and the minimum χ^2_{IP} of the two tracks in the final state $[\text{Min}(\chi^2_{\text{IP}})]$, for the same-sign sample and data sidebands in run 2.

particularly the two-body peaking backgrounds, but have almost no discriminating power on the semileptonic decay $\Lambda_b^0 \to p\mu^-\bar{\nu}_\mu$, which has the same visible final state particles as the signal channels. This decay represents the main physics background in this analysis. The $\Lambda_b^0 \to pX\mu^-\bar{\nu}_\mu$ decays with any additional unreconstructed particles (X) are expected to have negligible contribution in the fit region of $p\mu^-$ mass.

For the normalization channels, the selection for $B^0 \to K^+\pi^-$ candidates is the same as for the $B^0_{(s)} \to p\mu^-$ channel, except for the particle identification (PID) criteria. Similarly, the $B^+ \to J/\psi(\mu^+\mu^-)K^+$ candidate selection is also kept as similar as possible, applying the same selection used for the signal to the dimuon pair from the J/ψ decay. Additionally, loose quality requirements are applied on the J/ψ vertex, $\chi^2_{\text{vtx}} < 9$. Finally, a 100 MeV/c^2 mass window around the known B^+ mass and a 60 MeV/c^2 mass window around the known J/ψ mass [30] are used.

IV. MLP TRAINING AND CALIBRATION

A multilayer perceptron (MLP) [31] classifier implemented in the TMVA toolkit [32] is used to separate the $B^0_{(s)} \to p\mu^-$ signal from the combinatorial background, which arises from random combinations of tracks. The classifier is trained using a sample of simulated $B^0 \to p\mu^-$ events to describe the signal, and a data sample of same-sign $p\mu^+$ candidates to describe the combinatorial background. The same-sign sample reproduces the distributions of the MLP input variables from the data sidebands ($5067 < m_{p\mu^-} < 5100\,\text{MeV}/c^2$ or $5500 < m_{p\mu^-} < 5667\,\text{MeV}/c^2$). The following input variables are used: the minimum χ^2_{IP} of the two tracks in the final state and the χ^2_{IP} of the B^0 candidate, the vertex fit χ^2 of the B^0 decay and its displacement from the production vertex, the B^0 transverse momentum and its proper decay time, the distance of closest approach between the two tracks in the final state, the difference of pseudorapidity between the two final-state tracks, the angular difference between the direction of B^0 momentum and the direction defined by the secondary and primary vertices, and the angular

difference between the direction of the μ momentum and the vector perpendicular to the B^0 momentum and the beam axis in the B^0 rest frame. Distributions of two classifier input variables, the vertex fit χ^2 of the B^0 decay and the minimum χ^2_{IP} of the two tracks in the final state, for the same-sign sample and the data sidebands in run 2 are compared in Fig. 2.

The response of the MLP classifier is constructed to be uniform in the range [0,1] for signal after the full selection without PID requirements. For background, the MLP response peaks near zero. Its linear correlation with the $p\mu^-$ pair mass is below 1%. The MLP response is divided into eight intervals with boundaries of 0.0, 0.25, 0.4, 0.5, 0.6, 0.7, 0.8, 0.9, and 1.0. The MLP response is required to be greater than 0.25 in the final $p\mu^-$ mass distribution fit.

Since the MLP classifier is trained using only kinematic information of a two-body B^0 decay, its response is calibrated using $B^0 \to K^+\pi^-$ decays. To avoid biases, $B^0 \to K^+\pi^-$ candidates are selected from candidates where the trigger decision does not depend on the $B^0 \to K^+\pi^-$ candidates themselves. The number of $B^0 \to K^+\pi^-$ candidates in each interval of the MLP response is determined by fitting the $K^+\pi^-$ invariant mass distribution after the full selection. Furthermore, the candidates are corrected for PID efficiency and weighted to emulate the effect of the $B^0_{(s)} \to p\mu^-$ triggers. The distributions of the MLP response on $B^0 \to K^+\pi^-$ simulated samples and data samples show good agreement. The distribution of the MLP response from the $B^0 \to K^+\pi^-$ data samples is corrected by the ratio of the $B^0 \to p\mu^-$ and $B^0 \to K^+\pi^-$ MLP responses in simulated samples. The corrected MLP response is shown in Fig. 3 and regarded as the expected probability density function (PDF) of the MLP response for $B^0_{(s)} \to p\mu^-$ decays, due to negligible kinematic differences between the B^0 and B^0_s decays.

V. NORMALIZATION

The $B^0_{(s)} \to p\mu^-$ yields are obtained from a fit to the $p\mu^-$ invariant mass distribution and translated into
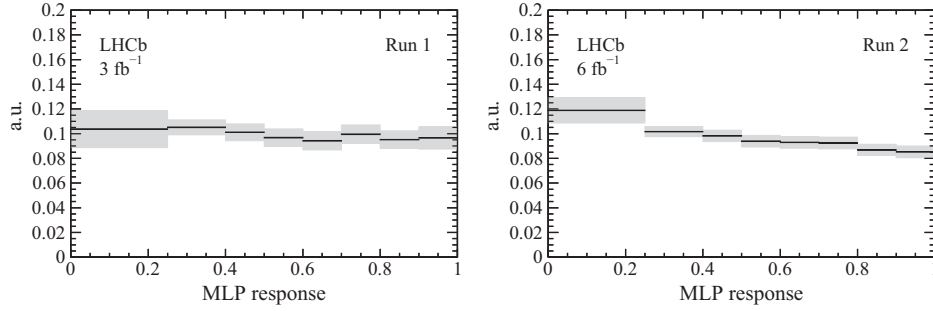
FIG. 3.   Expected distribution of the MLP response for $B^0_{(s)} \rightarrow p\mu^-$ decays as obtained from the $B^0 \rightarrow K^+\pi^-$ control channel, for (left) run 1 and (right) run 2 data. The total (statistical and systematic combined) uncertainty is shown as a light gray band, and the thickness of each horizontal line at the center indicates the statistical uncertainty. Each interval is normalized to its width.

branching fractions with the normalization channel $B^+ \rightarrow J/\psi(\mu^+\mu^-)K^+$, according to

$$\mathcal{B}(B^0_{(s)} \rightarrow p\mu^-) = \frac{f_{\text{norm}}}{f_{\text{sig}}} \frac{\epsilon_{\text{norm}}}{\epsilon_{\text{sig}}} \frac{N_{\text{sig}}}{N_{\text{norm}}} \mathcal{B}_{\text{norm}} \equiv \alpha_{\text{sig}} N_{\text{sig}}, \quad (1)$$

where $\mathcal{B}$, ϵ, and N are the branching fraction, efficiency, and yield of the corresponding channel and $f_{\text{sig(norm)}}$ indicates the fragmentation fraction of the relevant B meson. The parameter α_{sig} is the single-event sensitivity.

The $B^0 \rightarrow K^+\pi^-$ and $B^+ \rightarrow J/\psi(\mu^+\mu^-)K^+$ decays are used as control channels. The $B^0 \rightarrow K^+\pi^-$ mode is used as a proxy to determine the MLP PDF for signal channels (Sec. IV) and the $B^+ \rightarrow J/\psi(\mu^+\mu^-)K^+$ mode is used to extract the signal branching fraction. To validate the normalization procedure, the ratio between the measured branching fractions of $B^0 \rightarrow K^+\pi^-$ and $B^+ \rightarrow J/\psi(\mu^+\mu^-)K^+$ is determined as

$$\begin{aligned} R_{\text{norm}} &\equiv \frac{\mathcal{B}(B^0 \rightarrow K^+\pi^-)}{\mathcal{B}(B^+ \rightarrow J/\psi(\mu^+\mu^-)K^+)} \\ &= \frac{N_{B^0 \rightarrow K^+\pi^-} \times \varepsilon_{B^+ \rightarrow J/\psi(\mu^+\mu^-)K^+}}{N_{B^+ \rightarrow J/\psi(\mu^+\mu^-)K^+} \times \varepsilon_{B^0 \rightarrow K^+\pi^-}}, \end{aligned} \quad (2)$$

where ε and N are the selection efficiency and yield. Using the same fit models as in Ref. [33], the yields of the

normalization channels are obtained through fits to the mass distributions of the candidates separately for run 1 and run 2 datasets. The results of the fits are shown in Figs. 4 and 5.

The selection efficiency for signal and normalization channels includes efficiencies due to detector acceptance, tracking, reconstruction, trigger, and PID. All parts of the efficiency are evaluated using simulation, in which trigger and PID efficiencies are corrected using data [34,35].

Calibration samples where the trigger decision is independent of the candidate decay products are used to study the trigger efficiency. From these samples, $B^+ \rightarrow J/\psi(\mu^+\mu^-)K^+$ candidates are used to estimate the trigger efficiency for muons as a function of the muon p_T and IP. No proton trigger is used in this analysis. For the two normalization channels, $B^+ \rightarrow J/\psi(\mu^+\mu^-)K^+$ data samples are also used to determine the trigger efficiency map as a function of the B meson p_T. The resulting trigger efficiency maps are then applied to the simulation to determine the integrated trigger efficiency for a specific channel.

Particle identification efficiencies are evaluated using high-purity control samples of each particle species obtained from data [35,36]. These control samples are obtained by means of kinematic requirements only, with muons obtained from $J/\psi \rightarrow \mu^+\mu^-$ and $B^+ \rightarrow J/\psi K^+$ decays, pions and kaons from $D^0 \rightarrow K^-\pi^+$ decays selected
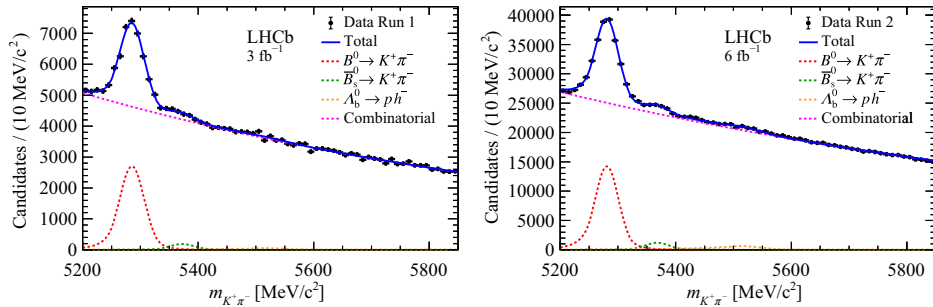

FIG. 4.   Mass distribution of $B^0 \rightarrow K^+\pi^-$ candidates in data for (left) run 1 and (right) run 2. The results of the invariant mass fits are superimposed.
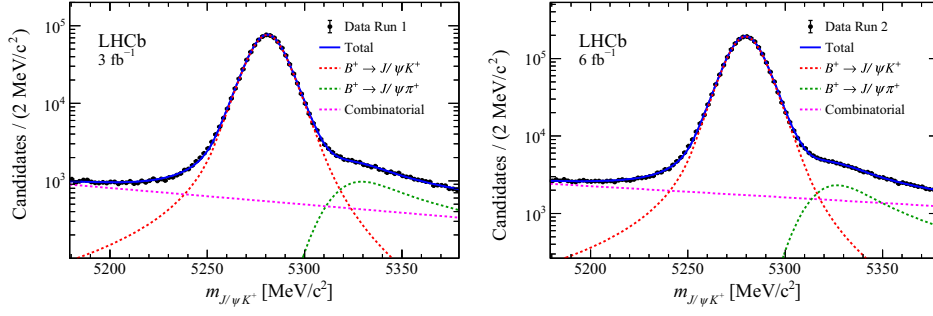
FIG. 5.   Mass distribution of $B^+ \to J/\psi K^+$ candidates in data for (left) run 1 and (right) run 2. The results of the invariant mass fits are superimposed.

via $D^{*+} \to D^0\pi^+$ decays, and protons from $\Lambda \to p\pi^-$ and $\Lambda_c^+ \to pK^-\pi^+$ decays. The muon PID efficiencies are evaluated as a function of the muon p_T and η. The PID efficiencies for different hadrons are evaluated as a function of p and η. The single-track efficiencies are then combined and averaged using the kinematic distributions of the corresponding simulated sample.

The ratios R_{norm} between the measured branching fractions of $B^0 \to K^+\pi^-$ and $B^+ \to J/\psi(\mu^+\mu^-)K^+$ in Eq. (2) are $R_{\mathrm{norm}} = 0.329 \pm 0.012$ and $R_{\mathrm{norm}} = 0.341 \pm 0.010$ for run 1 and run 2, respectively, where the uncertainties are statistical only and include the efficiency uncertainties from both channels. These values are in agreement with the ratio of the world averages of these branching fractions, $R_{\mathrm{PDG}} = 0.326 \pm 0.012$ [7].

VI. BACKGROUND CONTRIBUTIONS

In addition to the combinatorial background, the signal region is also potentially contaminated by background contributions from exclusive decays where one or more of the final-state particles are misidentified or not reconstructed. The most dangerous of these backgrounds are hadronic $X_b \to h^+h'^-$ decays—such as $B^0 \to K^+\pi^-$, $B_s^0 \to K^+K^-$, $B_s^0 \to K^+\pi^-$, $\Lambda_b^0 \to pK^-$, and $\Lambda_b^0 \to p\pi^-$— and partially reconstructed semileptonic decays—such as $\Lambda_b^0 \to p\mu^-\bar{\nu}_\mu$, $B_s^0 \to K^-\mu^+\nu_\mu$, and $B^0 \to \pi^-\mu^+\nu_\mu$. The partially reconstructed decays do not peak in the signal region but are potentially abundant. The expected number of candidates from each possible background decay that pass the signal selection is evaluated using simulation. The candidates from $B_{(s)}^0$ decays are normalized to the number of $B^+ \to J/\psi(\mu^+\mu^-)K^+$ decays found in data as

$$N_X = N_{B^+ \to J/\psi(\mu^+\mu^-)K^+} \cdot \frac{f_q}{f_u} \cdot \frac{\mathcal{B}(X)}{\mathcal{B}(B^+ \to J/\psi(\mu^+\mu^-)K^+)}$$
$$\cdot \frac{\epsilon(X)}{\epsilon(B^+ \to J/\psi(\mu^+\mu^-)K^+)}, \qquad (3)$$

where N_X is the expected number of candidates from the X decay that fall into the $B_{(s)}^0 \to p\mu^-$ signal mass window; $N_{B^+ \to J/\psi(\mu^+\mu^-)K^+}$ is the yield of $B^+ \to J/\psi(\mu^+\mu^-)K^+$ decays in the data; f_q is the fragmentation fraction for a b quark to produce either a meson with secondary quark content q or a baryon; and $\mathcal{B}$ and ϵ are the branching fraction and selection efficiency for a particular channel, respectively. For Λ_b^0 decays, the fragmentation fraction $f_{\Lambda_b^0}/f_d$ depends on the p_T of the Λ_b^0 baryon [37,38]. The $\Lambda_b^0 \to pK^-$ decay is used as a normalization channel to estimate the number of background Λ_b^0 candidates, thereby removing a potential bias due to the correlation between $f_{\Lambda_b^0}/f_d$ and p_T. The selection criteria on $\Lambda_b^0 \to pK^-$ candidates are largely the same as for the $B^0 \to K^+\pi^-$ normalization channel except for the p and K identification requirements.

The expected total number of $X_b \to h^+h'^-$ decays in the full MLP range is found to be negligible. The only background sources which are found to be relevant are the semileptonic decays $\Lambda_b^0 \to p\mu^-\bar{\nu}_\mu$, $B_s^0 \to K^-\mu^+\nu_\mu$, and $B^0 \to \pi^-\mu^+\nu_\mu$, with yields estimated to be roughly 8500 ± 2600, 50 ± 13 and 310 ± 16, respectively, for run 1 and 21000 ± 6400, 64 ± 17, and 410 ± 23, respectively, for run 2. The run 2 to run 1 yield ratios of $B_s^0 \to K^-\mu^+\nu_\mu$ and $B^0 \to \pi^-\mu^+\nu_\mu$ are considerably smaller than that of $\Lambda_b^0 \to p\mu^-\bar{\nu}_\mu$, which is mainly due to improved discrimination of protons from pions and kaons in run 2. These three decay modes are included in the final fit model.

VII. MEASUREMENT OF SIGNAL BRANCHING FRACTIONS

The branching fractions of the signal decays are determined using an unbinned extended maximum-likelihood fit to the $p\mu^-$ mass distributions, performed simultaneously on all the subsets. The fit is performed in the mass window $5067 < m_{p\mu^-} < 5667$ MeV/c^2. The full fit model in the data-taking period r and MLP interval i, $\mathrm{PDF}_{\mathrm{Full}}^{r,i}(m)$ is
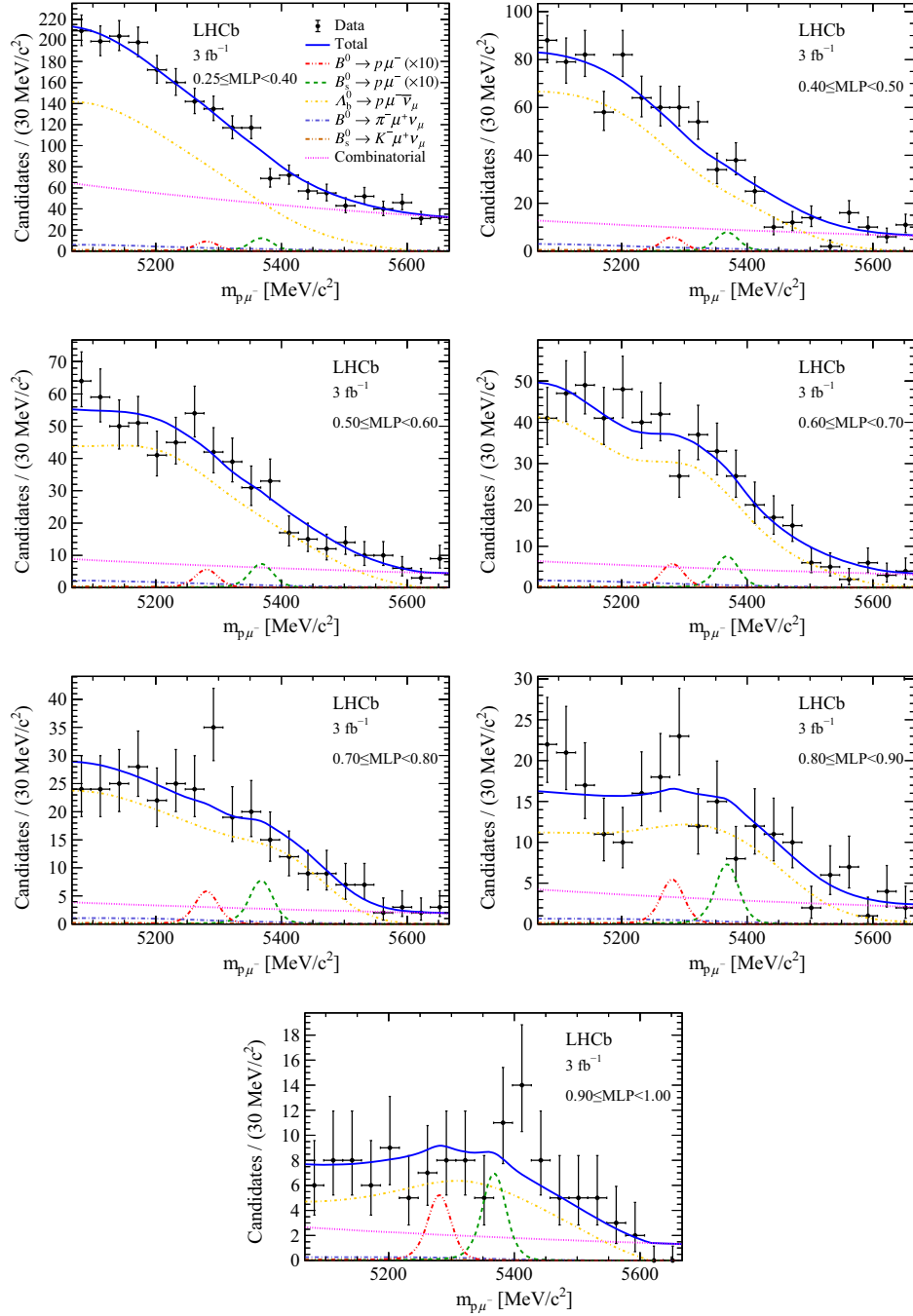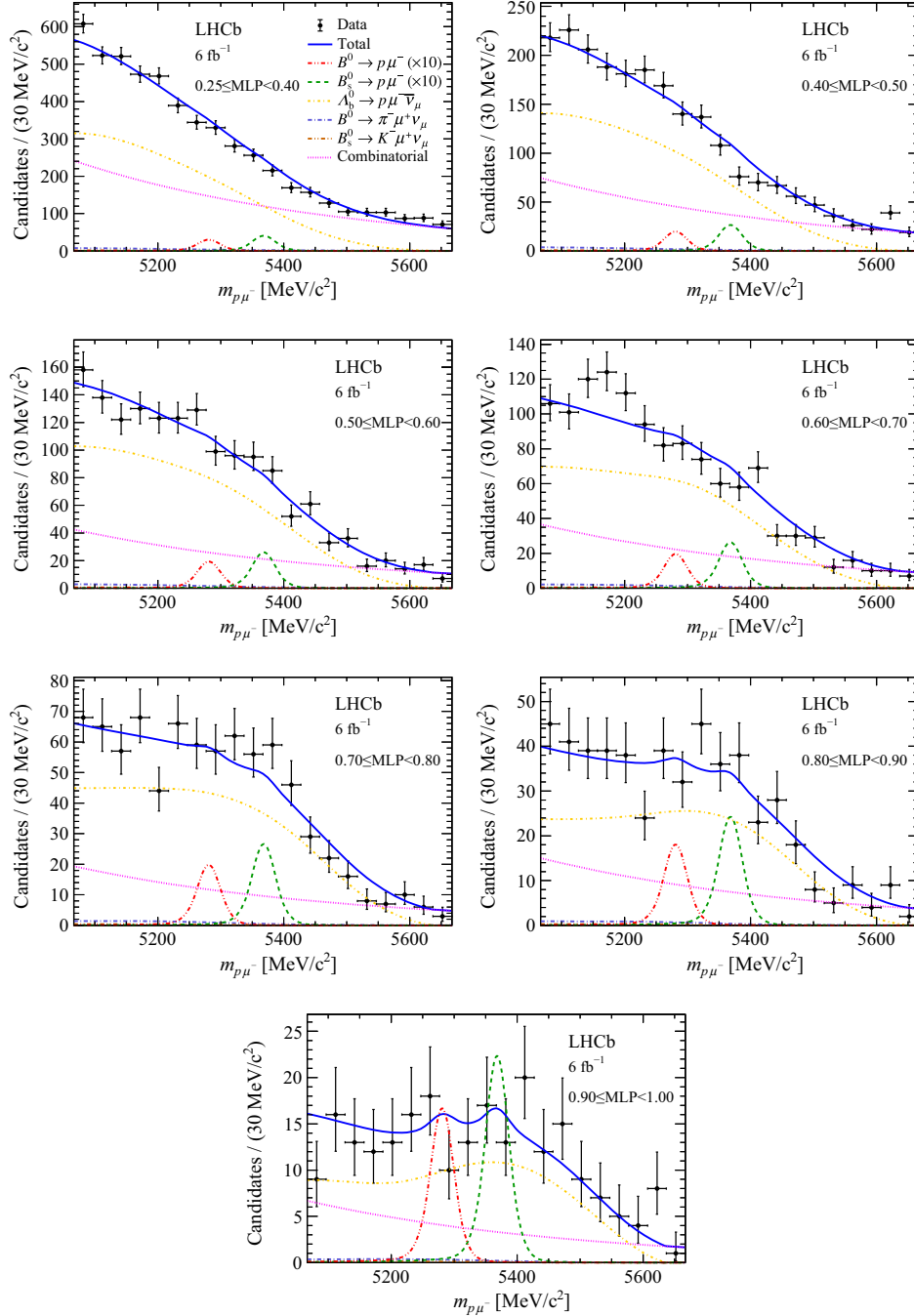
FIG. 6.   Mass distribution of signal candidates (black dots) for run 1 samples in regions of MLP. The results of the fit described in the text are also shown. The contributions from the two signal channels, $B^0 \to p\mu^-$ (red dashed lines) and $B_s^0 \to p\mu^-$ (green dashed lines), are scaled by a factor of 10 for better visibility.

$$\mathrm{PDF}_{\mathrm{Full}}^{r,i}(m) = \mathcal{P}\left(N_{\mathrm{meas}} | N_{\mathrm{com},r,i} + \sum_j N_{r,j} F_{r,i,j} + N_{\mathrm{sig},r,i}\right) \frac{1}{N_{\mathrm{com},r,i} + \sum_j N_{r,j} F_{r,i,j} + N_{\mathrm{sig},r,i}}$$

$$\times \left(N_{\mathrm{com},r,i}\mathrm{PDF}_{\mathrm{com},r}(m) + \sum_j N_{r,j} F_{r,i,j}\mathrm{PDF}_{r,i,j}(m) + N_{\mathrm{sig},r,i}\mathrm{PDF}_{\mathrm{sig}}(m)\right), \tag{4}$$

FIG. 7. Mass distribution of signal candidates (black dots) for run 2 samples in regions of MLP. The results of the fit described in the text are also shown. The contributions from the two signal channels, $B^0 \to p\mu^-$ (red dashed lines) and $B_s^0 \to p\mu^-$ (green dashed lines), are scaled by a factor of 10 for better visibility.

where $\mathcal{P}$ is the Poisson probability of measuring N, given the fitted yields. The signal model, denoted PDF_{sig}, is described in detail below. Also $\text{PDF}_{\text{com},r}$ is the PDF for combinatorial background, which is described with an exponential function with an independent shape parameter in each data-taking period and independent yield $N_{\text{com},r,i}$ in each subset. $\text{PDF}_{r,i,j}$ represents the PDF for the physical

background with index j, which is modeled based on histograms determined from simulation and smoothed with a second order interpolation. $N_{r,j}$ and $F_{r,i,j}$ represent the expected yield and the yield fraction in each subset for physical backgrounds.

PDF_{sig} is a sum of a double-sided crystal ball function [39] and a Gaussian function. The signal shape
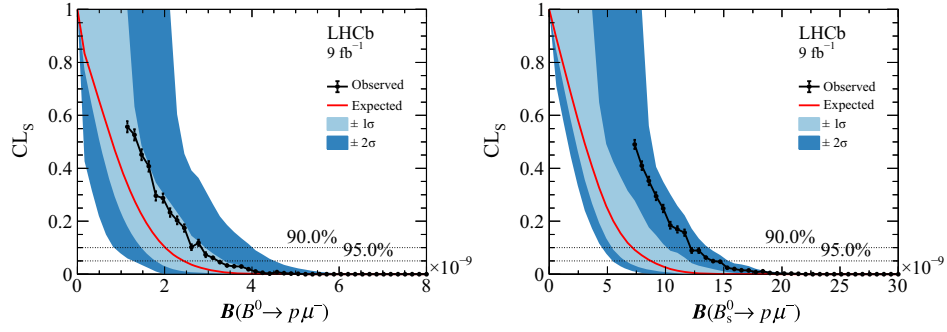
FIG. 8. Results from the CLs scan used to obtain the limit on (left) $\mathcal{B}(B^0 \to p\mu^-)$ and (right) $\mathcal{B}(B_s^0 \to p\mu^-)$. The background-only expectation is shown by the red line and the 1σ and 2σ bands are shown as light blue and blue bands, respectively. The observation is shown as the solid black line. The two dashed lines intersecting with the observation indicate the limits at 90% and 95% CL for the upper and lower line, respectively.

parameters are obtained from simulation, with data-driven scale factors applied to the core resolution to correct for minor data-simulation discrepancies. For this purpose, since there is no appropriate control channel with a proton and a muon in the final state, $\Lambda_b^0 \to pK^-$ and $J/\psi \to \mu^+\mu^-$ decays are analyzed comparing the invariant mass resolution in data and simulation. The results are then combined to reproduce the effect on an $p\mu^-$ final state. Corrections to the mass resolution are of the order of 10%. The mass shape parameters are found to be independent of the particular MLP interval and only two models, for the run 1 and run 2 data samples, are used.

The yield in each subset, $N_{\text{sig},r,i}$, is expressed as

$$N_{\text{sig},r,i} = \frac{\mathcal{B}_{\text{sig}} f_{\text{sig}} \varepsilon_{\text{PID},r,i} \varepsilon_{\text{others},r} F_{\text{sig},r,i} N_{\text{norm},r}}{\mathcal{B}_{\text{norm}} f_{\text{norm}} \varepsilon_{\text{norm},r}}. \quad (5)$$

Here, $\mathcal{B}$ and f represent the branching fraction and fragmentation fraction of the signal channel or the normalization channel. The quantities $N_{\text{norm},r}$ and $\varepsilon_{\text{norm},r}$ are the yield and efficiency of the normalization mode $B^+ \to J/\psi(\mu^+\mu^-)K^+$. Furthermore, $\varepsilon_{\text{PID},r,i}$ and $\varepsilon_{\text{others},r}$ are the PID efficiency and the total efficiency without the PID requirements for signal channels. $F_{r,i,j}$ represents the fraction in each subset for signal channels (Fig. 3). The quantities $\mathcal{B}_{\text{sig}}$ and $N_{\text{com},r,i}$ are free to vary in the fit, while f_{sig}, $N_{\text{norm},r}$, $\mathcal{B}_{\text{norm}}$, f_{norm}, $\varepsilon_{\text{norm},r}$, $N_{r,j}$, $F_{r,i,j}$, $\varepsilon_{\text{PID},r,i}$, $\varepsilon_{\text{others},r}$, $F_{\text{sig},r,i}$, and $N_{\text{norm},r}$ are Gaussian constrained, according to the expected value and uncertainty.

The result of the fit in each subset is shown in Figs. 6 and 7. The resulting branching fractions are

$$\mathcal{B}(B^0 \to p\mu^-) = (0.84 \pm 1.17 \pm 0.57) \times 10^{-9},$$

$$\mathcal{B}(B_s^0 \to p\mu^-) = (4.28 \pm 3.99 \pm 2.29) \times 10^{-9},$$

where the first uncertainty is statistical and the second systematic. No significant excess of $B^0 \to p\mu^-$ or

$B_s^0 \to p\mu^-$ decays is observed and upper limits on the branching fractions are set using the CLs method [40] with a one-sided test statistic [41] as implemented in Refs. [42,43]. The one-sided test statistic for a given branching fraction value is defined as twice the negative logarithm of the profile likelihood ratio if it is larger than the measured branching fraction and zero otherwise. Its distribution is determined from pseudoexperiments, where nuisance parameters are set to their best fit values when generating pseudoexperiments. The central values of the Gaussian constraints are independently varied within their uncertainties for each pseudoexperiment as described in Ref. [44]. With the inclusion of systematic effects as discussed below, the CLs curves as a function of the branching ratios are shown in Fig. 8, and the upper limits at 90 (95)% confidence level (CL) are reported in Table I, where the observed upper limits are both above the expected ones. This is likely due to a fluctuation of the concentration of $\Lambda_b^0 \to p\mu^-\bar{\nu}_\mu$ events around the known $B_{(s)}^0$ masses in MLP regions with large MLP response values.

Several systematic uncertainties can affect the evaluation of the limit on the $B^0 \to p\mu^-$ and $B_s^0 \to p\mu^-$ branching fractions through the normalization formula [Eq. (1)]. The systematic uncertainties considered are related to the fraction of signal and physical backgrounds in each MLP interval; expected total yields of physical backgrounds; signal efficiency; mass resolution of signal shape; fragmentation fraction $f_{\text{sig}}/f_{\text{norm}}$ (only applicable for the B_s^0

TABLE I. Expected and observed upper limits for $\mathcal{B}(B^0 \to p\mu^-)$ and $\mathcal{B}(B_s^0 \to p\mu^-)$ at 90% (95%) CL, with systematic effects included. No signal is assumed for the expected upper limits.

Channel	Expected	Observed
$B^0 \to p\mu^-$	$1.9(2.4) \times 10^{-9}$	$2.6(3.1) \times 10^{-9}$
$B_s^0 \to p\mu^-$	$7.0(8.6) \times 10^{-9}$	$12.1(14.0) \times 10^{-9}$

mode); branching fraction, efficiency and yield of the normalization channel $B^+ \to J/\psi(\mu^+\mu^-)K^+$. The systematic uncertainties on the efficiencies of the signal and normalization channels include the uncertainties arising from modeling the dependencies of the trigger (PID) efficiency maps. The effect on the $p\mu^-$ mass distribution and yield fraction from $\Lambda_b^0 \to p\mu^-\bar{\nu}_\mu$ form factor uncertainty and different $\Lambda_b^0 \to p\mu^-\bar{\nu}_\mu$ physics models have been studied and found to be negligible. No systematic uncertainty is assigned due to the assumptions of unpolarized final states. These systematic uncertainties are taken into account for the limit computation by constraining the respective parameters in the likelihood fit with a Gaussian distribution having the central value of the parameter as the mean and its uncertainty as the width. The overall impact on the limits is evaluated to be 4% on $B^0 \to p\mu^-$ and 11% on $B_s^0 \to p\mu^-$.

VIII. SUMMARY

In summary, a search for the LNV and BNV decays $B^0 \to p\mu^-$ and $B_s^0 \to p\mu^-$ is performed using the full run 1 and run 2 data samples of the LHCb experiment, using a sample of proton-proton collision data corresponding to a total integrated luminosity of 9 fb^{-1}. No excesses are observed for these two modes and upper limits on the branching fractions are set to be $\mathcal{B}(B^0 \to p\mu^-) < 2.6(3.1) \times 10^{-9}$ and $\mathcal{B}(B_s^0 \to p\mu^-) < 12.1(14.0) \times 10^{-9}$ at 90% (95%) CL These results represent the first upper limits on these decays to date.

[1] A. D. Sakharov, Violation of *CP* invariance, C asymmetry, and baryon asymmetry of the universe, Pis'ma Zh. Eksp. Teor. Fiz. **5**, 32 (1967).

[2] H. Georgi and S. L. Glashow, Unity of All Elementary-Particle Forces, Phys. Rev. Lett. **32**, 438 (1974).

[3] H. Fritzsch and P. Minkowski, Unified interactions of leptons and hadrons, Ann. Phys. (N.Y.) **93**, 193 (1975).

[4] F. Gursey, P. Ramond, and P. Sikivie, A universal gauge theory model based on E6, Phys. Lett. **60B**, 177 (1976).

[5] S. M. Barr, A new symmetry breaking pattern for SO(10) and proton decay, Phys. Lett. **112B**, 219 (1982).

[6] J. P. Derendinger, J. E. Kim, and D. V. Nanopoulos, Anti-SU(5), Phys. Lett. **139B**, 170 (1984).

[7] P. A. Zyla *et al.* (Particle Data Group), Review of particle physics, Prog. Theor. Exp. Phys. **2020**, 083C01 (2020).

[8] R. Godang *et al.* (CLEO Collaboration), Search for baryon and lepton number violating decays of the tau lepton, Phys. Rev. D **59**, 091303 (1999).

[9] M. E. McCracken *et al.*, Search for baryon-number and lepton-number violating decays of Λ hyperons using the CLAS detector at Jefferson Laboratory, Phys. Rev. D **92**, 072002 (2015).

[10] M. Ablikim *et al.* (BESIII Collaboration), Search for baryon and lepton number violating decay $D^\pm \to n(\bar{n})e^\pm$, Phys. Rev. D **106**, 112009 (2022).

[11] M. Ablikim *et al.* (BESIII Collaboration), Search for baryon- and lepton-number violating decays $D^0 \to \bar{p}e^+$ and $D^0 \to pe^-$, Phys. Rev. D **105**, 032006 (2022).

[12] M. Ablikim *et al.* (BESIII Collaboration), Search for baryon and lepton number violating decays $D^+ \to \bar{\Lambda}(\bar{\Sigma}^0)e^+$ and $D^+ \to \Lambda(\Sigma^0)e^+$, Phys. Rev. D **101**, 031102 (2020).

[13] M. Ablikim *et al.* (BESIII Collaboration), Search for baryon and lepton number violation in $J/\psi \to \Lambda_c^+ e^- + c.c.$, Phys. Rev. D **99**, 072006 (2019).

[14] P. del Amo Sanchez *et al.* (*BABAR* Collaboration), Searches for the baryon- and lepton-number violating decays $B^0 \to \Lambda_c^+ \ell^-$, $B^- \to \Lambda \ell^-$, and $B^- \to \bar{\Lambda} \ell^-$, Phys. Rev. D **83**, 091101 (2011).

[15] W.-S. Hou, M. Nagashima, and A. Soddu, Baryon number violation involving higher generations, Phys. Rev. D **72**, 095001 (2005).

[16] A. A. Alves Jr. *et al.* (LHCb Collaboration), The LHCb detector at the LHC, J. Instrum. **3**, S08005 (2008).

[17] R. Aaij *et al.* (LHCb Collaboration), LHCb detector performance, Int. J. Mod. Phys. A **30**, 1530022 (2015).

[18] R. Aaij *et al.*, The LHCb trigger and its performance in 2011, J. Instrum. **8**, P04022 (2013).

[19] V. V. Gligorov and M. Williams, Efficient, reliable and fast high-level triggering using a bonsai boosted decision tree, J. Instrum. **8**, P02013 (2013).

[20] T. Likhomanenko, P. Ilten, E. Khairullin, A. Rogozhnikov, A. Ustyuzhanin, and M. Williams, LHCb topological trigger reoptimization, J. Phys. Conf. Ser. **664**, 082025 (2015).

[21] T. Sjöstrand, S. Mrenna, and P. Skands, A brief introduction to PYTHIA 8.1, Comput. Phys. Commun. **178**, 852 (2008).

[22] I. Belyaev *et al.* (LHCb Collaboration), Handling of the generation of primary events in Gauss, the LHCb simulation framework, J. Phys. Conf. Ser. **331**, 032047 (2011).

[23] D. J. Lange, The EvtGen particle decay simulation package, Nucl. Instrum. Methods Phys. Res., Sect. A **462**, 152 (2001).

[24] P. Golonka and Z. Was, PHOTOS Monte Carlo: A precision tool for QED corrections in Z and W decays, Eur. Phys. J. C **45**, 97 (2006).

[25] J. Allison *et al.* (Geant4 Collaboration), Geant4 developments and applications, IEEE Trans. Nucl. Sci. **53**, 270 (2006).

[26] S. Agostinelli *et al.* (GEANT4 Collaboration), Geant4—a simulation toolkit, Nucl. Instrum. Methods Phys. Res., Sect. A **506**, 250 (2003).

[27] M. Clemencic, G. Corti, S. Easo, C. R. Jones, S. Miglioranzi, M. Pappagallo, and P. Robbe (LHCb Collaboration), The LHCb simulation application, Gauss: Design, evolution and experience, J. Phys. Conf. Ser. **331**, 032023 (2011).

[28] R. Aaij *et al.* (LHCb Collaboration), Measurement of the $B_s^0 \to \mu^+\mu^-$ decay properties and search for the $B^0 \to \mu^+\mu^-$ and $B_s^0 \to \mu^+\mu^-\gamma$ decays, Phys. Rev. D **105**, 012010 (2022).

[29] F. Archilli *et al.*, Performance of the muon identification at LHCb, J. Instrum. **8**, P10020 (2013).

[30] P. A. Zyla *et al.* (Particle Data Group), Review of particle physics, Prog. Theor. Exp. Phys. **2020**, 083C01 (2020).

[31] A. Hoecker *et al.*, TMVA 4—Toolkit for multivariate data analysis with ROOT. Users Guide, arXiv:physics/0703039.

[32] H. Voss, A. Hoecker, J. Stelzer, and F. Tegenfeldt, TMVA—Toolkit for multivariate data analysis with ROOT, Proc. Sci. ACAT2007 (**2007**) 040.

[33] R. Aaij *et al.* (LHCb Collaboration), Measurement of the $B_s^0 \to \mu^+\mu^-$ decay properties and search for the $B^0 \to \mu^+\mu^-$ and $B_s^0 \to \mu^+\mu^-\gamma$ decays, Phys. Rev. D **105**, 012010 (2022).

[34] S. Tolk, J. Albrecht, F. Dettori, and A. Pellegrino, Data driven trigger efficiency determination at LHCb, Report No. LHCb-PUB-2014-039, 2014.

[35] L. Anderlini *et al.*, The PIDCalib package, Report No. LHCb-PUB-2016-021, 2016.

[36] R. Aaij *et al.*, Selection and processing of calibration samples to measure the particle identification performance of the LHCb experiment in Run 2, EPJ Tech. Instrum. **6**, 1 (2019).

[37] R. Aaij *et al.* (LHCb Collaboration), Study of the kinematic dependences of Λ_b^0 production in pp collisions and a measurement of the $\Lambda_b^0 \to \Lambda_c^+ \pi^-$ branching fraction, J. High Energy Phys. 08 (2014) 143.

[38] R. Aaij *et al.* (LHCb Collaboration), Measurement of b hadron fractions in 13 TeV pp collisions, Phys. Rev. D **100**, 031102 (2019).

[39] T. Skwarnicki, A study of the radiative cascade transitions between the Upsilon-prime and Upsilon resonances, Ph.D thesis, Institute of Nuclear Physics, Krakow, 1986.

[40] A. L. Read, Presentation of search results: The CLs technique, J. Phys. G **28**, 2693 (2002).

[41] G. Cowan, K. Cranmer, E. Gross, and O. Vitells, Asymptotic formulae for likelihood-based tests of new physics, Eur. Phys. J. C **71**, 1554 (2011); **73**, 2501(E) (2013).

[42] M. Kenzie *et al.*, GammaCombo: A statistical analysis framework for combining measurements, fitting datasets and producing confidence intervals, 10.5281/zenodo.3371421.

[43] R. Aaij *et al.* (LHCb Collaboration), Measurement of the CKM angle γ from a combination of LHCb results, J. High Energy Phys. 12 (2016) 087.

[44] S. Bodhisattva, M. Walker, and M. Woodroofe, On the unified method with nuisance parameters, Statistica Sinica **19**, 301 (2009), https://www.jstor.org/stable/24308721.

R. Aaij,[32] A. S. W. Abdelmotteleb,[50] C. Abellan Beteta,[44] F. Abudinén,[50] T. Ackernley,[54] B. Adeva,[40] M. Adinolfi,[48] H. Afsharnia,[9] C. Agapopoulou,[13] C. A. Aidala,[77] S. Aiola,[25] Z. Ajaltouni,[9] S. Akar,[59] K. Akiba,[32] J. Albrecht,[15] F. Alessio,[42] M. Alexander,[53] A. Alfonso Albero,[39] Z. Aliouche,[56] P. Alvarez Cartelle,[49] R. Amalric,[13] S. Amato,[2] J. L. Amey,[48] Y. Amhis,[11,42] L. An,[42] L. Anderlini,[22] M. Andersson,[44] A. Andreianov,[38] M. Andreotti,[21] D. Andreou,[62] D. Ao,[6] F. Archilli,[17] A. Artamonov,[38] M. Artuso,[62] E. Aslanides,[10] M. Atzeni,[44] B. Audurier,[12] S. Bachmann,[17] M. Bachmayer,[43] J. J. Back,[50] A. Bailly-reyre,[13] P. Baladron Rodriguez,[40] V. Balagura,[12] W. Baldini,[21] J. Baptista de Souza Leite,[1] M. Barbetti,[22,b] R. J. Barlow,[56] S. Barsuk,[11] W. Barter,[55] M. Bartolini,[49] F. Baryshnikov,[38] J. M. Basels,[14] G. Bassi,[29,c] B. Batsukh,[4] A. Battig,[15] A. Bay,[43] A. Beck,[50] M. Becker,[15] F. Bedeschi,[29] I. B. Bediaga,[1] A. Beiter,[62] V. Belavin,[38] S. Belin,[40] V. Bellee,[44] K. Belous,[38] I. Belov,[38] I. Belyaev,[38] G. Benane,[10] G. Bencivenni,[23] E. Ben-Haim,[13] A. Berezhnoy,[38] R. Bernet,[44] S. Bernet Andres,[75] D. Berninghoff,[17] H. C. Bernstein,[62] C. Bertella,[56] A. Bertolin,[28] C. Betancourt,[44] F. Betti,[42] Ia. Bezshyiko,[44] S. Bhasin,[48] J. Bhom,[35] L. Bian,[68] M. S. Bieker,[15] N. V. Biesuz,[21] S. Bifani,[47] P. Billoir,[13] A. Biolchini,[32] M. Birch,[55] F. C. R. Bishop,[49] A. Bitadze,[56] A. Bizzeti, M. P. Blago,[49]

T. Blake[50] F. Blanc[43] S. Blusk[62] D. Bobulska[53] J. A. Boelhauve[15] O. Boente Garcia[12] T. Boettcher[59]
A. Boldyrev[38] C. S. Bolognani[74] R. Bolzonella[21,d] N. Bondar[38,42] F. Borgato[28] S. Borghi[56] M. Borsato[17]
J. T. Borsuk[35] S. A. Bouchiba[43] T. J. V. Bowcock[54] A. Boyer[42] C. Bozzi[21] M. J. Bradley[55] S. Braun[60]
A. Brea Rodriguez[40] J. Brodzicka[35] A. Brossa Gonzalo[40] J. Brown[54] D. Brundu[27] A. Buonaura[44]
L. Buonincontri[28] A. T. Burke[56] C. Burr[42] A. Bursche[66] A. Butkevich[38] J. S. Butter[32] J. Buytaert[42]
W. Byczynski[42] S. Cadeddu[27] H. Cai[68] R. Calabrese[21,d] L. Calefice[15] S. Cali[23] R. Calladine[47] M. Calvi[26,e]
M. Calvo Gomez[75] P. Campana[23] D. H. Campora Perez[74] A. F. Campoverde Quezada[6] S. Capelli[26,e]
L. Capriotti[20,f] A. Carbone[20,f] G. Carboni[31] R. Cardinale[24,g] A. Cardini[27] I. Carli[4] P. Carniti[26,e] L. Carus[14]
A. Casais Vidal[40] R. Caspary[17] G. Casse[54] M. Cattaneo[42] G. Cavallero[42] V. Cavallini[21,d] S. Celani[43]
J. Cerasoli[10] D. Cervenkov[57] A. J. Chadwick[54] M. G. Chapman[48] M. Charles[13] Ph. Charpentier[42]
C. A. Chavez Barajas[54] M. Chefdeville[8] C. Chen[3] S. Chen[4] A. Chernov[35] S. Chernyshenko[46]
V. Chobanova[40] S. Cholak[43] M. Chrzaszcz[35] A. Chubykin[38] V. Chulikov[38] P. Ciambrone[23] M. F. Cicala[50]
X. Cid Vidal[40] G. Ciezarek[42] G. Ciullo[21,d] P. E. L. Clarke[52] M. Clemencic[42] H. V. Cliff[49] J. Closier[42]
J. L. Cobbledick[56] V. Coco[42] J. A. B. Coelho[11] J. Cogan[10] E. Cogneras[9] L. Cojocariu[37] P. Collins[42]
T. Colombo[42] L. Congedo[19] A. Contu[27] N. Cooke[47] I. Corredoira[40] G. Corti[42] B. Couturier[42]
D. C. Craik[58] J. Crkovská[61] M. Cruz Torres[1,h] R. Currie[52] C. L. Da Silva[61] S. Dadabaev[38] L. Dai[65]
X. Dai[5] E. Dall'Occo[15] J. Dalseno[40] C. D'Ambrosio[42] J. Daniel[9] A. Danilina[38] P. d'Argent[15]
J. E. Davies[56] A. Davis[56] O. De Aguiar Francisco[56] J. de Boer[42] K. De Bruyn[73] S. De Capua[56]
M. De Cian[43] U. De Freitas Carneiro Da Graca[1] E. De Lucia[23] J. M. De Miranda[1] L. De Paula[2] M. De Serio[19,i]
D. De Simone[44] P. De Simone[23] F. De Vellis[15] J. A. de Vries[74] C. T. Dean[61] F. Debernardis[19,i] D. Decamp[8]
V. Dedu[10] L. Del Buono[13] B. Delaney[58] H.-P. Dembinski[15] V. Denysenko[44] O. Deschamps[9] F. Dettori[27,j]
B. Dey[71] A. Di Cicco[23] P. Di Nezza[23] I. Diachkov[38] S. Didenko[38] L. Dieste Maronas[40] S. Ding[62]
V. Dobishuk[46] A. Dolmatov[38] C. Dong[3] A. M. Donohoe[18] F. Dordei[27] A. C. dos Reis[1] L. Douglas[53]
A. G. Downes[8] M. W. Dudek[35] L. Dufour[42] V. Duk[72] P. Durante[42] J. M. Durham[61] D. Dutta[56]
A. Dziurda[35] A. Dzyuba[38] S. Easo[51] U. Egede[63] V. Egorychev[38] S. Eidelman[38,a] C. Eirea Orro[40]
S. Eisenhardt[52] E. Ejopu[56] S. Ek-In[43] L. Eklund[76] S. Ely[62] A. Ene[37] E. Epple[61] S. Escher[14] J. Eschle[44]
S. Esen[44] T. Evans[56] F. Fabiano[27,j] L. N. Falcao[1] Y. Fan[6] B. Fang[68] S. Farry[54] D. Fazzini[26,e] M. Feo[42]
M. Fernandez Gomez[40] A. D. Fernez[60] F. Ferrari[20] L. Ferreira Lopes[43] F. Ferreira Rodrigues[2]
S. Ferreres Sole[32] M. Ferrillo[44] M. Ferro-Luzzi[42] S. Filippov[38] R. A. Fini[19] M. Fiorini[21,d] M. Firlej[34]
K. M. Fischer[57] D. S. Fitzgerald[77] C. Fitzpatrick[56] T. Fiutowski[34] F. Fleuret[12] M. Fontana[13] F. Fontanelli[24,g]
R. Forty[42] D. Foulds-Holt[49] V. Franco Lima[54] M. Franco Sevilla[60] M. Frank[42] E. Franzoso[21,d] G. Frau[17]
C. Frei[42] D. A. Friday[53] J. Fu[6] Q. Fuehring[15] T. Fulghesu[13] E. Gabriel[32] G. Galati[19,i] M. D. Galati[73]
A. Gallas Torreira[40] D. Galli[20,f] S. Gambetta[52,42] Y. Gan[3] M. Gandelman[2] P. Gandini[25] Y. Gao[5]
M. Garau[27,j] L. M. Garcia Martin[50] P. Garcia Moreno[39] J. García Pardiñas[26,e] B. Garcia Plana,[40]
F. A. Garcia Rosales[12] L. Garrido[39] C. Gaspar[42] R. E. Geertsema[32] D. Gerick[17] L. L. Gerken[15]
E. Gersabeck[56] M. Gersabeck[56] T. Gershon[50] L. Giambastiani[28] V. Gibson[49] H. K. Giemza[36]
A. L. Gilman[57] M. Giovannetti[23,k] A. Gioventù[40] P. Gironella Gironell[39] C. Giugliano[21,d] M. A. Giza[35]
K. Gizdov[52] E. L. Gkougkousis[42] V. V. Gligorov[13,42] C. Göbel[64] E. Golobardes[75] D. Golubkov[38]
A. Golutvin[55,38] A. Gomes[1,l] S. Gomez Fernandez[39] F. Goncalves Abrantes[57] M. Goncerz[35] G. Gong[3]
I. V. Gorelov[38] C. Gotti[26] J. P. Grabowski[17] T. Grammatico[13] L. A. Granado Cardoso[42] E. Graugés[39]
E. Graverini[43] G. Graziani, A. T. Grecu[37] L. M. Greeven[32] N. A. Grieser[4] L. Grillo[53] S. Gromov[38]
B. R. Gruberg Cazon[57] C. Gu[3] M. Guarise[21,d] M. Guittiere[11] P. A. Günther[17] E. Gushchin[38] A. Guth[14]
Y. Guz[38] T. Gys[42] T. Hadavizadeh[63] G. Haefeli[43] C. Haen[42] J. Haimberger[42] S. C. Haines[49]
T. Halewood-leagas[54] M. M. Halvorsen[42] P. M. Hamilton[60] J. Hammerich[54] Q. Han[7] X. Han[17]
E. B. Hansen[56] S. Hansmann-Menzemer[17,42] L. Hao[6] N. Harnew[57] T. Harrison[54] C. Hasse[42] M. Hatch[42]
J. He[6,m] K. Heijhoff[32] K. Heinicke[15] C. Henderson[59] R. D. L. Henderson[63,50] A. M. Hennequin[58]
K. Hennessy[54] L. Henry[42] J. Herd[55] J. Heuel[14] A. Hicheur[2] D. Hill[43] M. Hilton[56] S. E. Hollitt[15]
J. Horswill[56] R. Hou[7] Y. Hou[8] J. Hu[17] J. Hu[66] W. Hu[5] X. Hu[3] W. Huang[6] X. Huang[68] W. Hulsbergen[32]
R. J. Hunter[50] M. Hushchyn[38] D. Hutchcroft[54] P. Ibis[15] M. Idzik[34] D. Ilin[38] P. Ilten[59] A. Inglessi[38]

A. Iniukhin[38], A. Ishteev[38], K. Ivshin[38], R. Jacobsson[42], H. Jage[14], S. J. Jaimes Elles[41], S. Jakobsen[42], E. Jans[32], B. K. Jashal[41], A. Jawahery[60], V. Jevtic[15], E. Jiang[60], X. Jiang[4,6], Y. Jiang[6], M. John[57], D. Johnson[58], C. R. Jones[49], T. P. Jones[50], B. Jost[42], N. Jurik[42], I. Juszczak[35], S. Kandybei[45], Y. Kang[3], M. Karacson[42], D. Karpenkov[38], M. Karpov[38], J. W. Kautz[59], F. Keizer[42], D. M. Keller[62], M. Kenzie[50], T. Ketel[32], B. Khanji[15], A. Kharisova[38], S. Kholodenko[38,38], G. Khreich[11], T. Kirn[14], V. S. Kirsebom[43], O. Kitouni[58], S. Klaver[33], N. Kleijne[29,c], K. Klimaszewski[36], M. R. Kmiec[36], S. Koliiev[46], A. Kondybayeva[38], A. Konoplyannikov[38], P. Kopciewicz[34], R. Kopecna[17], P. Koppenburg[32], M. Korolev[38], I. Kostiuk[32,46], O. Kot[46], S. Kotriakhova, A. Kozachuk[38], P. Kravchenko[38], L. Kravchuk[38], R. D. Krawczyk[42], M. Kreps[50], S. Kretzschmar[14], P. Krokovny[38,38], W. Krupa[34], W. Krzemien[36], J. Kubat[17], W. Kucewicz[35,34], M. Kucharczyk[35], V. Kudryavtsev[38,38], G. J. Kunde[61], A. Kupsc[76], D. Lacarrere[42], G. Lafferty[56], A. Lai[27], A. Lampis[27,j], D. Lancierini[44], C. Landesa Gomez[40], J. J. Lane[56], R. Lane[48], G. Lanfranchi[23], C. Langenbruch[14], J. Langer[15], O. Lantwin[38], T. Latham[50], F. Lazzari[29,n], M. Lazzaroni[25,o], R. Le Gac[10], S. H. Lee[77], R. Lefèvre[9], A. Leflat[38], S. Legotin[38], P. Lenisa[21,d], O. Leroy[10], T. Lesiak[35], B. Leverington[17], A. Li[3], H. Li[66], K. Li[7], P. Li[17], P.-R. Li[67], S. Li[7], T. Li[66], Y. Li[4], Z. Li[62], X. Liang[62], C. Lin[6], T. Lin[51], R. Lindner[42], V. Lisovskyi[15], R. Litvinov[27,j], G. Liu[66], H. Liu[6], Q. Liu[6], S. Liu[4,6], A. Lobo Salvia[39], A. Loi[27], R. Lollini[72], J. Lomba Castro[40], I. Longstaff[53], J. H. Lopes[2], A. Lopez Huertas[39], S. López Soliño[40], G. H. Lovell[49], Y. Lu[4,p], C. Lucarelli[22,b], D. Lucchesi[28,q], S. Luchuk[38], M. Lucio Martinez[74], V. Lukashenko[32,46], Y. Luo[3], A. Lupato[56], E. Luppi[21,d], A. Lusiani[29,c], K. Lynch[18], X.-R. Lyu[6], L. Ma[4], R. Ma[6], S. Maccolini[20], F. Machefert[11], F. Maciuc[37], I. Mackay[57], V. Macko[43], P. Mackowiak[15], L. R. Madhan Mohan[48], A. Maevskiy[38], D. Maisuzenko[38], M. W. Majewski[34], J. J. Malczewski[35], S. Malde[57], B. Malecki[35,42], A. Malinin[38], T. Maltsev[38,38], G. Manca[27,j], G. Mancinelli[10], C. Mancuso[11,25,o], D. Manuzzi[20], C. A. Manzari[44], D. Marangotto[25,o], J. F. Marchand[8], U. Marconi[20], S. Mariani[22,b], C. Marin Benito[39], J. Marks[17], A. M. Marshall[48], P. J. Marshall[54], G. Martelli[72,r], G. Martellotti[30], L. Martinazzoli[42,e], M. Martinelli[26,e], D. Martinez Santos[40], F. Martinez Vidal[41], A. Massafferri[1], M. Materok[14], R. Matev[42], A. Mathad[44], V. Matiunin[38], C. Matteuzzi[26], K. R. Mattioli[77], A. Mauri[32], E. Maurice[12], J. Mauricio[39], M. Mazurek[42], M. McCann[55], L. Mcconnell[18], T. H. McGrath[56], N. T. McHugh[53], A. McNab[56], R. McNulty[18], J. V. Mead[54], B. Meadows[59], G. Meier[15], D. Melnychuk[36], S. Meloni[26,e], M. Merk[32,74], A. Merli[25,o], L. Meyer Garcia[2], D. Miao[4,6], M. Mikhasenko[70,s], D. A. Milanes[69], E. Millard[50], M. Milovanovic[42], M.-N. Minard[8,8,a], A. Minotti[26,e], T. Miralles[9], S. E. Mitchell[52], B. Mitreska[56], D. S. Mitzel[15], A. Mödden[15], R. A. Mohammed[57], R. D. Moise[14], S. Mokhnenko[38], T. Mombächer[40], M. Monk[50,63], I. A. Monroy[69], S. Monteil[9], M. Morandin[28], G. Morello[23], M. J. Morello[29,c], J. Moron[34], A. B. Morris[70], A. G. Morris[50], R. Mountain[62], H. Mu[3], E. Muhammad[50], F. Muheim[52], M. Mulder[73], K. Müller[44], C. H. Murphy[57], D. Murray[56], R. Murta[55], P. Muzzetto[27,j], P. Naik[48], T. Nakada[43], R. Nandakumar[51], T. Nanut[42], I. Nasteva[2], M. Needham[52], N. Neri[25,o], S. Neubert[70], N. Neufeld[42], P. Neustroev[38], R. Newcombe[55], J. Nicolini[15,11], E. M. Niel[43], S. Nieswand[14], N. Nikitin[38], N. S. Nolte[58], C. Normand[8,27,j], J. Novoa Fernandez[40], C. Nunez[77], A. Oblakowska-Mucha[34], V. Obraztsov[38], T. Oeser[14], D. P. O'Hanlon[48], S. Okamura[21,d], R. Oldeman[27,j], F. Oliva[52], M. E. Olivares[62], C. J. G. Onderwater[73], R. H. O'Neil[52], J. M. Otalora Goicochea[2], T. Ovsiannikova[38], P. Owen[44], A. Oyanguren[41], O. Ozcelik[52], K. O. Padeken[70], B. Pagare[50], P. R. Pais[42], T. Pajero[57], A. Palano[19], M. Palutan[23], Y. Pan[56], G. Panshin[38], L. Paolucci[50], A. Papanestis[51], M. Pappagallo[19,i], L. L. Pappalardo[21,d], C. Pappenheimer[59], W. Parker[60], C. Parkes[56], B. Passalacqua[21,d], G. Passaleva[22], A. Pastore[19], M. Patel[55], C. Patrignani[20,f], C. J. Pawley[74], A. Pearce[42], A. Pellegrino[32], M. Pepe Altarelli[42], S. Perazzini[20], D. Pereima[38], A. Pereiro Castro[40], P. Perret[9], M. Petric[53], K. Petridis[48], A. Petrolini[24,g], A. Petrov[38], S. Petrucci[52], M. Petruzzo[25], H. Pham[62], A. Philippov[38], R. Piandani[6], L. Pica[29,c], M. Piccini[72], B. Pietrzyk[8], G. Pietrzyk[11], M. Pili[57], D. Pinci[30], F. Pisani[42], M. Pizzichemi[26,42,e], V. Placinta[37], J. Plews[47], M. Plo Casasus[40], F. Polci[13,42], M. Poli Lener[23], M. Poliakova[62], A. Poluektov[10], N. Polukhina[38,38], I. Polyakov[42], E. Polycarpo[2], S. Ponce[42], D. Popov[6,42], S. Popov[38], S. Poslavskii[38], K. Prasanth[35], L. Promberger[42], C. Prouve[40], V. Pugatch[46], V. Puill[11], G. Punzi[29,t], H. R. Qi[3], W. Qian[6], N. Qin[3], S. Qu[3], R. Quagliani[43], N. V. Raab[18], R. I. Rabadan Trejo[6], B. Rachwal[34], J. H. Rademacker[48], R. Rajagopalan[62], M. Rama[29], M. Ramos Pernas[50], M. S. Rangel[2], F. Ratnikov[38,38], G. Raven[33,42], M. Rebollo De Miguel[41], F. Redi[42], J. Reich[48], F. Reiss[56], C. Remon Alepuz[41], Z. Ren[3],

V. Renaudin[57] P. K. Resmi[10] R. Ribatti[29,c] A. M. Ricci[27] S. Ricciardi[51] K. Richardson[58] M. Richardson-Slipper[52] K. Rinnert[54] P. Robbe[11] G. Robertson[52] A. B. Rodrigues[43] E. Rodrigues[54] E. Rodriguez Fernandez[40] J. A. Rodriguez Lopez[69] E. Rodriguez Rodriguez[40] A. Rollings[57] P. Roloff[42] V. Romanovskiy[38] M. Romero Lamas[40] A. Romero Vidal[40] J. D. Roth[77,a] M. Rotondo[23] M. S. Rudolph[62] T. Ruf[42] R. A. Ruiz Fernandez[40] J. Ruiz Vidal[41] A. Ryzhikov[38] J. Ryzka[34] J. J. Saborido Silva[40] N. Sagidova[38] N. Sahoo[47] B. Saitta[27,j] M. Salomoni[42] C. Sanchez Gras[32] I. Sanderswood[41] R. Santacesaria[30] C. Santamarina Rios[40] M. Santimaria[23] E. Santovetti[31,k] D. Saranin[38] G. Sarpis[14] M. Sarpis[70] A. Sarti[30] C. Satriano[30,u] A. Satta[31] M. Saur[15] D. Savrina[38,38] H. Sazak[9] L. G. Scantlebury Smead[57] A. Scarabotto[13] S. Schael[14] S. Scherl[54] M. Schiller[53] H. Schindler[42] M. Schmelling[16] B. Schmidt[42] S. Schmitt[14] O. Schneider[43] A. Schopper[42] M. Schubiger[32] S. Schulte[43] M. H. Schune[11] R. Schwemmer[42] B. Sciascia[23,42] A. Sciuccati[42] S. Sellam[40] A. Semennikov[38] M. Senghi Soares[33] A. Sergi[24,g] N. Serra[44] L. Sestini[28] A. Seuthe[15] Y. Shang[5] D. M. Shangase[77] M. Shapkin[38] I. Shchemerov[38] L. Shchutska[43] T. Shears[54] L. Shekhtman[38,38] Z. Shen[5] S. Sheng[4,6] V. Shevchenko[38] B. Shi[6] E. B. Shields[26,e] Y. Shimizu[11] E. Shmanin[38] J. D. Shupperd[62] B. G. Siddi[21,d] R. Silva Coutinho[44] G. Simi[28] S. Simone[19,i] M. Singla[63] N. Skidmore[56] R. Skuza[17] T. Skwarnicki[62] M. W. Slater[47] J. C. Smallwood[57] J. G. Smeaton[49] E. Smith[44] K. Smith[61] M. Smith[55] A. Snoch[32] L. Soares Lavra[9] M. D. Sokoloff[59] F. J. P. Soler[53] A. Solomin[38,48] A. Solovev[38] I. Solovyev[38] R. Song[63] F. L. Souza De Almeida[2] B. Souza De Paula[2] B. Spaan[15,a] E. Spadaro Norella[25,o] E. Spiridenkov[38] P. Spradlin[53] V. Sriskaran[42] F. Stagni[42] M. Stahl[59] S. Stahl[42] S. Stanislaus[57] E. N. Stein[42] O. Steinkamp[44] O. Stenyakin[38] H. Stevens[15] S. Stone[62,a] D. Strekalina[38] F. Suljik[57] J. Sun[27] L. Sun[68] Y. Sun[60] P. Svihra[56] P. N. Swallow[47] K. Swientek[34] A. Szabelski[36] T. Szumlak[34] M. Szymanski[42] Y. Tan[3] S. Taneja[56] A. R. Tanner[48] M. D. Tat[57] A. Terentev[38] F. Teubert[42] E. Thomas[42] D. J. D. Thompson[47] K. A. Thomson[54] H. Tilquin[55] V. Tisserand[9] S. T'Jampens[8] M. Tobin[4] L. Tomassetti[21,d] G. Tonani[25,o] X. Tong[5] D. Torres Machado[1] D. Y. Tou[3] E. Trifonova[38] S. M. Trilov[48] C. Trippl[43] G. Tuci[6] A. Tully[43] N. Tuning[32] A. Ukleja[36] D. J. Unverzagt[17] E. Ursov[38] A. Usachov[32] A. Ustyuzhanin[38,38] U. Uwer[17] A. Vagner[38] V. Vagnoni[20] A. Valassi[42] G. Valenti[20] N. Valls Canudas[75] M. van Beuzekom[32] M. Van Dijk[43] H. Van Hecke[61] E. van Herwijnen[38] C. B. Van Hulse[40,v] M. van Veghel[73] R. Vazquez Gomez[39] P. Vazquez Regueiro[40] C. Vázquez Sierra[42] S. Vecchi[21] J. J. Velthuis[48] M. Veltri[22,w] A. Venkateswaran[43] M. Veronesi[32] M. Vesterinen[50] D. Vieira[59] M. Vieites Diaz[43] X. Vilasis-Cardona[75] E. Vilella Figueras[54] A. Villa[20] P. Vincent[13] F. C. Volle[11] D. vom Bruch[10] A. Vorobyev[38] V. Vorobyev[38] N. Voropaev[38] K. Vos[74] C. Vrahas[52] R. Waldi[17] J. Walsh[29] G. Wan[5] C. Wang[17] J. Wang[5] J. Wang[4] J. Wang[3] J. Wang[68] M. Wang[5] R. Wang[48] X. Wang[66] Y. Wang[7] Z. Wang[44] Z. Wang[3] Z. Wang[6] J. A. Ward[50,63] N. K. Watson[47] D. Websdale[55] Y. Wei[5] C. Weisser[58] B. D. C. Westhenry[48] D. J. White[56] M. Whitehead[53] A. R. Wiederhold[50] D. Wiedner[15] G. Wilkinson[57] M. K. Wilkinson[59] I. Williams[49] M. Williams[58] M. R. J. Williams[52] R. Williams[49] F. F. Wilson[51] W. Wislicki[36] M. Witek[35] L. Witola[17] C. P. Wong[61] G. Wormser[11] S. A. Wotton[49] H. Wu[62] K. Wyllie[42] Z. Xiang[6] D. Xiao[7] Y. Xie[7] A. Xu[5] J. Xu[6] L. Xu[3] L. Xu[3] M. Xu[50] Q. Xu[6] Z. Xu[9] Z. Xu[6] D. Yang[3] S. Yang[6] Y. Yang[6] Z. Yang[5] Z. Yang[60] L. E. Yeomans[54] V. Yeroshenko[11] H. Yeung[56] H. Yin[7] J. Yu[65] X. Yuan[62] E. Zaffaroni[43] M. Zavertyaev[16] M. Zdybal[35] O. Zenaiev[42] M. Zeng[3] C. Zhang[5] D. Zhang[7] L. Zhang[3] S. Zhang[65] S. Zhang[5] Y. Zhang[5] Y. Zhang[57] A. Zharkova[38] A. Zhelezov[17] Y. Zheng[6] T. Zhou[5] X. Zhou[6] Y. Zhou[6] V. Zhovkovska[11] X. Zhu[3] X. Zhu[7] Z. Zhu[6] V. Zhukov[14,38] Q. Zou[4,6] S. Zucchelli[20,f] D. Zuliani[28] and G. Zunica[56]

(LHCb Collaboration)

[1]*Centro Brasileiro de Pesquisas Físicas (CBPF), Rio de Janeiro, Brazil*
[2]*Universidade Federal do Rio de Janeiro (UFRJ), Rio de Janeiro, Brazil*
[3]*Center for High Energy Physics, Tsinghua University, Beijing, China*
[4]*Institute Of High Energy Physics (IHEP), Beijing, China*
[5]*School of Physics State Key Laboratory of Nuclear Physics and Technology,
Peking University, Beijing, China*

[6]University of Chinese Academy of Sciences, Beijing, China

[7]Institute of Particle Physics, Central China Normal University, Wuhan, Hubei, China

[8]Université Savoie Mont Blanc, CNRS, IN2P3-LAPP, Annecy, France

[9]Université Clermont Auvergne, CNRS/IN2P3, LPC, Clermont-Ferrand, France

[10]Aix Marseille Univ, CNRS/IN2P3, CPPM, Marseille, France

[11]Université Paris-Saclay, CNRS/IN2P3, IJCLab, Orsay, France

[12]Laboratoire Leprince-Ringuet, CNRS/IN2P3, Ecole Polytechnique, Institut Polytechnique de Paris, Palaiseau, France

[13]LPNHE, Sorbonne Université, Paris Diderot Sorbonne Paris Cité, CNRS/IN2P3, Paris, France

[14]I. Physikalisches Institut, RWTH Aachen University, Aachen, Germany

[15]Fakultät Physik, Technische Universität Dortmund, Dortmund, Germany

[16]Max-Planck-Institut für Kernphysik (MPIK), Heidelberg, Germany

[17]Physikalisches Institut, Ruprecht-Karls-Universität Heidelberg, Heidelberg, Germany

[18]School of Physics, University College Dublin, Dublin, Ireland

[19]INFN Sezione di Bari, Bari, Italy

[20]INFN Sezione di Bologna, Bologna, Italy

[21]INFN Sezione di Ferrara, Ferrara, Italy

[22]INFN Sezione di Firenze, Firenze, Italy

[23]INFN Laboratori Nazionali di Frascati, Frascati, Italy

[24]INFN Sezione di Genova, Genova, Italy

[25]INFN Sezione di Milano, Milano, Italy

[26]INFN Sezione di Milano-Bicocca, Milano, Italy

[27]INFN Sezione di Cagliari, Monserrato, Italy

[28]Università degli Studi di Padova, Università e INFN, Padova, Padova, Italy

[29]INFN Sezione di Pisa, Pisa, Italy

[30]INFN Sezione di Roma La Sapienza, Roma, Italy

[31]INFN Sezione di Roma Tor Vergata, Roma, Italy

[32]Nikhef National Institute for Subatomic Physics, Amsterdam, Netherlands

[33]Nikhef National Institute for Subatomic Physics and VU University Amsterdam, Amsterdam, Netherlands

[34]AGH - University of Science and Technology, Faculty of Physics and Applied Computer Science, Kraków, Poland

[35]Henryk Niewodniczanski Institute of Nuclear Physics Polish Academy of Sciences, Kraków, Poland

[36]National Center for Nuclear Research (NCBJ), Warsaw, Poland

[37]Horia Hulubei National Institute of Physics and Nuclear Engineering, Bucharest-Magurele, Romania

[38]Affiliated with an institute covered by a cooperation agreement with CERN

[39]ICCUB, Universitat de Barcelona, Barcelona, Spain

[40]Instituto Galego de Física de Altas Enerxías (IGFAE), Universidade de Santiago de Compostela, Santiago de Compostela, Spain

[41]Instituto de Fisica Corpuscular, Centro Mixto Universidad de Valencia - CSIC, Valencia, Spain

[42]European Organization for Nuclear Research (CERN), Geneva, Switzerland

[43]Institute of Physics, Ecole Polytechnique Fédérale de Lausanne (EPFL), Lausanne, Switzerland

[44]Physik-Institut, Universität Zürich, Zürich, Switzerland

[45]NSC Kharkiv Institute of Physics and Technology (NSC KIPT), Kharkiv, Ukraine

[46]Institute for Nuclear Research of the National Academy of Sciences (KINR), Kyiv, Ukraine

[47]University of Birmingham, Birmingham, United Kingdom

[48]H.H. Wills Physics Laboratory, University of Bristol, Bristol, United Kingdom

[49]Cavendish Laboratory, University of Cambridge, Cambridge, United Kingdom

[50]Department of Physics, University of Warwick, Coventry, United Kingdom

[51]STFC Rutherford Appleton Laboratory, Didcot, United Kingdom

[52]School of Physics and Astronomy, University of Edinburgh, Edinburgh, United Kingdom

[53]School of Physics and Astronomy, University of Glasgow, Glasgow, United Kingdom

[54]Oliver Lodge Laboratory, University of Liverpool, Liverpool, United Kingdom

[55]Imperial College London, London, United Kingdom

[56]Department of Physics and Astronomy, University of Manchester, Manchester, United Kingdom

[57]Department of Physics, University of Oxford, Oxford, United Kingdom

[58]Massachusetts Institute of Technology, Cambridge, Massachusetts, USA

[59]University of Cincinnati, Cincinnati, Ohio, USA

[60]University of Maryland, College Park, Maryland, USA

[61]Los Alamos National Laboratory (LANL), Los Alamos, New Mexico, USA

[62]Syracuse University, Syracuse, New York, USA

[63]*School of Physics and Astronomy, Monash University, Melbourne, Australia*
(associated with Institution Department of Physics, University of Warwick, Coventry, United Kingdom)
[64]*Pontifícia Universidade Católica do Rio de Janeiro (PUC-Rio), Rio de Janeiro, Brazil*
(associated with Institution Universidade Federal do Rio de Janeiro (UFRJ), Rio de Janeiro, Brazil)
[65]*Physics and Micro Electronic College, Hunan University, Changsha City, China*
(associated with Institution Institute of Particle Physics, Central China Normal University,
Wuhan, Hubei, China)
[66]*Guangdong Provincial Key Laboratory of Nuclear Science, Guangdong-Hong Kong Joint Laboratory of*
Quantum Matter, Institute of Quantum Matter, South China Normal University, Guangzhou, China
(associated with Institution Center for High Energy Physics, Tsinghua University, Beijing, China)
[67]*Lanzhou University, Lanzhou, China*
(associated with Institution Institute Of High Energy Physics (IHEP), Beijing, China)
[68]*School of Physics and Technology, Wuhan University, Wuhan, China*
(associated with Institution Center for High Energy Physics, Tsinghua University, Beijing, China)
[69]*Departamento de Fisica, Universidad Nacional de Colombia, Bogota, Colombia*
(associated with Institution LPNHE, Sorbonne Université, Paris Diderot Sorbonne Paris Cité,
CNRS/IN2P3, Paris, France)
[70]*Universität Bonn - Helmholtz-Institut für Strahlen und Kernphysik, Bonn, Germany*
(associated with Institution Physikalisches Institut, Ruprecht-Karls-Universität Heidelberg,
Heidelberg, Germany)
[71]*Eotvos Lorand University, Budapest, Hungary*
(associated with Institution European Organization for Nuclear Research (CERN), Geneva, Switzerland)
[72]*INFN Sezione di Perugia, Perugia, Italy*
(associated with Institution INFN Sezione di Ferrara, Ferrara, Italy)
[73]*Van Swinderen Institute, University of Groningen, Groningen, Netherlands*
(associated with Institution Nikhef National Institute for Subatomic Physics, Amsterdam, Netherlands)
[74]*Universiteit Maastricht, Maastricht, Netherlands*
(associated with Institution Nikhef National Institute for Subatomic Physics, Amsterdam, Netherlands)
[75]*DS4DS, La Salle, Universitat Ramon Llull, Barcelona, Spain*
(associated with Institution ICCUB, Universitat de Barcelona, Barcelona, Spain)
[76]*Department of Physics and Astronomy, Uppsala University, Uppsala, Sweden*
(associated with Institution School of Physics and Astronomy, University of Glasgow,
Glasgow, United Kingdom)
[77]*University of Michigan, Ann Arbor, Michigan, USA*
(associated with Institution Syracuse University, Syracuse, New York, USA)

[a]Deceased.
[b]Also at Università di Firenze, Firenze, Italy.
[c]Also at Scuola Normale Superiore, Pisa, Italy.
[d]Also at Università di Ferrara, Ferrara, Italy.
[e]Also at Università di Milano Bicocca, Milano, Italy.
[f]Also at Università di Bologna, Bologna, Italy.
[g]Also at Università di Genova, Genova, Italy.
[h]Also at Universidad Nacional Autónoma de Honduras, Tegucigalpa, Honduras.
[i]Also at Università di Bari, Bari, Italy.
[j]Also at Università di Cagliari, Cagliari, Italy.
[k]Also at Università di Roma Tor Vergata, Roma, Italy.
[l]Also at Universidade de Brasília, Brasília, Brazil.
[m]Also at Hangzhou Institute for Advanced Study, UCAS, Hangzhou, China.
[n]Also at Università di Siena, Siena, Italy.
[o]Also at Università degli Studi di Milano, Milano, Italy.
[p]Also at Central South U., Changsha, China.
[q]Also at Università di Padova, Padova, Italy.
[r]Also at Università di Perugia, Perugia, Italy.
[s]Also at Excellence Cluster ORIGINS, Munich, Germany.
[t]Also at Università di Pisa, Pisa, Italy.
[u]Also at Università della Basilicata, Potenza, Italy.
[v]Also at Universidad de Alcalá, Alcalá de Henares, Spain.
[w]Also at Università di Urbino, Urbino, Italy.